Available online at www.sciencedirect.com

ScienceDirect

Procedia Structural Integrity 24 (2019) 746–757

Structural Integrity Procedia

www.elsevier.com/locate/procedia

AIAS 2019 International Conference on Stress Analysis

Numerical Investigation on the Influence of Tightening in Bolted Joints

Greco A.[a], De Luca A.[a], Lamanna G.[a]*, Sepe R.[b]

[a]*Department of Engineering, University of Campania Luigi Vanvitelli, via Roma 29, Aversa, Italy*
[b] *Department of Chemical, Materials and Industrial Production Engineering, University of Naples Federico II, Piazzale V. Tecchio 80, Neaples, Italy*

Abstract

In a bolted joint, the preload level resulting from the tightening torque represents a very important parameter governing the stresses distributions involving the joint under the real loading conditions. This paper deals with the development of a Finite Element (FE) model for the investigation of the effects of some selected preload levels on the stress-strain states affecting both bolt and plate in a single lap joint. The aim of this FE model is to support the design phase of strain gauges instrumented bolt to evaluate experimentally the rate of tensile load applied to the joint that the bolt absorbs with different preloads. The test article consists of two steel plates, a steel bolt and an aluminum nut. The results herein presented showed firstly that, without bolt preload, the tensile load applied to the joint is completely transferred to the bolt and that the load transferred to the bolt almost linearly decreases as the preload increases. Moreover, at a selected preload level, the transversal and longitudinal stresses (with respect to the load direction) increase as the tensile load increases, while the stress along the plate thickness direction decreases, reaching negative values. On the other hand, at a selected tensile load level, the transversal and longitudinal stresses as well as the stress along the thickness direction decrease as the preload level increases. Predicting the mechanical behaviour of the only bolted joint, if the same bolt model will be used to simulate the mechanical behaviour in a hybrid single-lap joint, possible imperfections of the model will have to certainly be linked to the modelling of the adhesive.

Keywords: Bolted joints; tightening torque; numerical modeling.

* Corresponding author. Tel.: +39-081-5010-419; fax: +39-081-5010-295.
E-mail address: giuseppe.lamanna@unicampania.it

10.1016/j.prostr.2020.02.066

1. Introduction

Bolted joints are widely used in several industrial fields such as mechanical engineering, aerospace, automotive engineering and so on. Being non-permanent mechanical joints, they allow the connection disassembly without resorting to destructive methods.

An inadequate design may cause undesired accidents, so bolted connections need to have a high level of detailing compatible with the design requirements. Moreover, these types of connections have the main drawback due to drilled holes causing stress and strain concentration, increasing the risk of crack initiation and propagation (Chakherlou and Abazadeh (2012), Chakherlou et al. (2011)).

Many studies focused on the possibility to improve the strength of bolted joints by using adhesives (Lamanna et al. (2014)). Hybrid (bolted-bonded) joints can be used to improve the efficiency and the strength of bolted joints, allowing the loads to be transmitted through both the fastener and the adhesive layer. In order to investigate on the mechanical behavior and to design hybrid joints, it is necessary to evaluate the load transferred through the fastener and the adhesive, before sizing the whole assembly behavior. In particular, to predict the strength of the bolted joint, several studies about the shear failure of the bolt have to be carried out.

Several numerical models, mainly based on the Finite Element (FE) method, have been proposed in literature to approach this problem. Kelly (2005) studied the load distribution in hybrid composite single lap joints by using a 3D FE model in order to investigate the effects of joint design parameters on the load transferred by the bolt. Kelly, (2006) considering also a CFRP (Carbon Fiber Reinforced Polymers) adherent. Samaei et al. (2016) investigated, both experimentally and numerically, the effects of tightening torque on the fatigue crack growth rate and stress intensity factors in a cracked hybrid single lap joint.

Armentani et al. (2017) studied the structural behaviour of a single lap hybrid composite joint subjected to a tensile external load by means of FE model, while De Luca et al. (2018) investigated numerically, by means of a FE model, and experimentally the stress relaxation phenomena in composite-metal bolted joints. Sawa et al. (2015) and Shirakawa et al. (2018) investigated numerically on the mechanical characteristics of bolted circular flange joints and the stress analysis at the bearing surfaces in bolted joints under external loading respectively.

Similar studies have been proposed by McCarthy et al. (2005), Hoang-Ngoc and Paroissien (2010) and Aldaş and Sen (2013) that used 3D FE analyses for investigating the mechanical behaviour of hybrid joints.

In brief, about the literature until 2011, He (2011) proposed a systematic review about the FE analyses of bonded and hybrid joints. In addition to FE methods, alternative methods have been developed for the study of the mechanical behaviour of hybrid joints. Barut and Madenci (2009) developed a semi-analytical method to evaluate the stresses in the laminates, adhesive, and bolt when the bolt is pretensioned to produce a clamp-up force effect while the joint is subjected to external loading and prescribed displacement constraints. Bois et al. (2013) provided a semi-analytical 1-D model for predicting the strength of a hybrid bolted joint.

Atta et al. (2019) demonstrated the goodness of two numerical models, based on FE and Artificial Neural Networks (ANNs) methods, in predicting the failure stages of double lap bolted joint, by comparing their results with those ones provided by experimental tests.

However, many of the numerical models proposed in literature aimed to simulate the structural behaviour of hybrid joints, in spite of provide good levels of accuracy in terms of hybrid joint failure, do not demonstrate the reliability to evaluate the load transferred to the bolt in the hybrid joint.

In this paper a homemade instrumented bolt has been analysed by FE analyses. In this way, it has been possible to assess the effectiveness of the modelled bolt. It means that, when the same bolt model will be used, in future investigations, to simulate the mechanical behaviour in hybrid single-lap joints, possible imperfections of the model will have to be linked to the modelling of the adhesive.

2. Test article

The bolted single-lap joint consists of two steel plates (142.5 mm x 35 mm x 5.225 mm sized), a steel bolt and an aluminum nut in the middle, as schematically shown in Fig. 1.

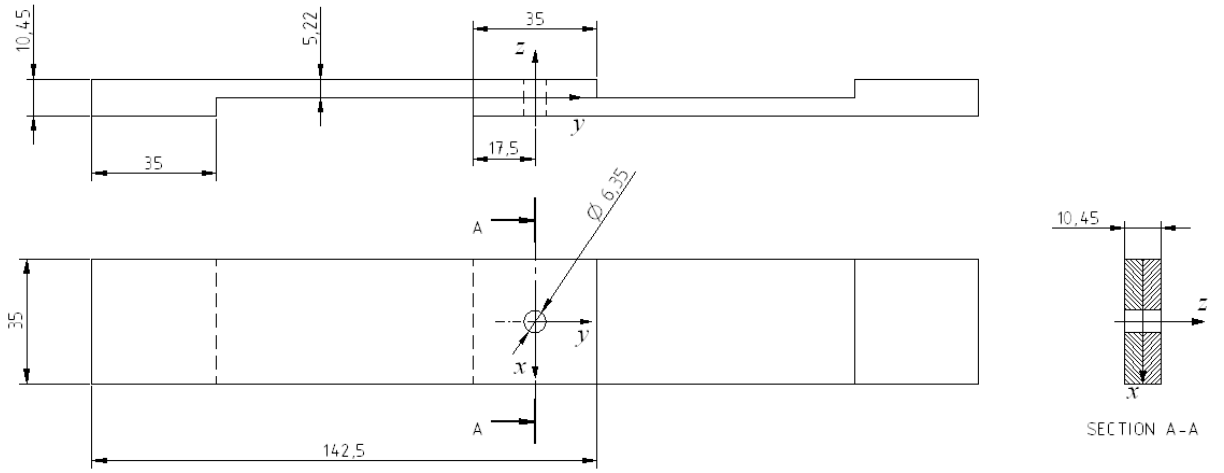

Fig. 1. Shape and dimensions (in mm) of the single lap joint.

The bolt designed for the joint is based on the Hi-Lok® by Lisi Aerospace (Fig. 2), whose dimensions are reported in Table 1.

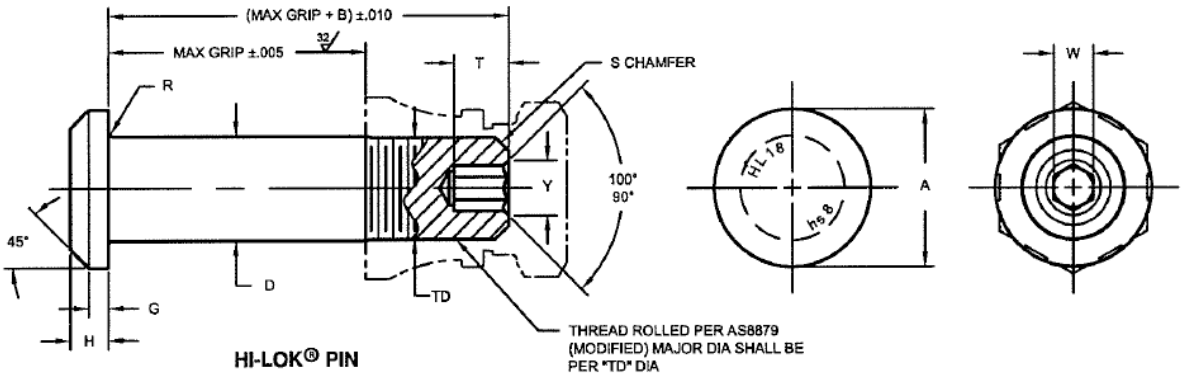

Fig. 2. Hi-Lok Pin by Lisi Aerospace.

Table 1. Dimensions of Hi Lok pin.

Pin nom. diameter D [mm]		A [mm]	B [mm]	D [mm]	TD [mm]	G [mm]	H [mm]	R [mm]	S CHAMFER	SOCKET W [mm]	SOCKET T [mm]	SOCKET Y [mm]	THREAD
6.35	min.	9.83	10.03	6.31	6.12	7.62	14.99	3.81	0.79 mm x 45°	2.40	3.30	3.10	¼-28UNJF-3A Modified
	max.	10.46		6.34	6.19		17.52	6.35		2.45	3.81	3.60	

Fig. 3 shows the geometry of the new bolt. The bolt is characterized by a shaft keyway where the strain gauges are installed. Moreover, a hexagonal head has been added in order to simplify the installation and the tightening of the bolt for the tests.

The bolt is made of 36NiCrMo16 hardened and tempered steel with shank diameter of 6.35 mm.

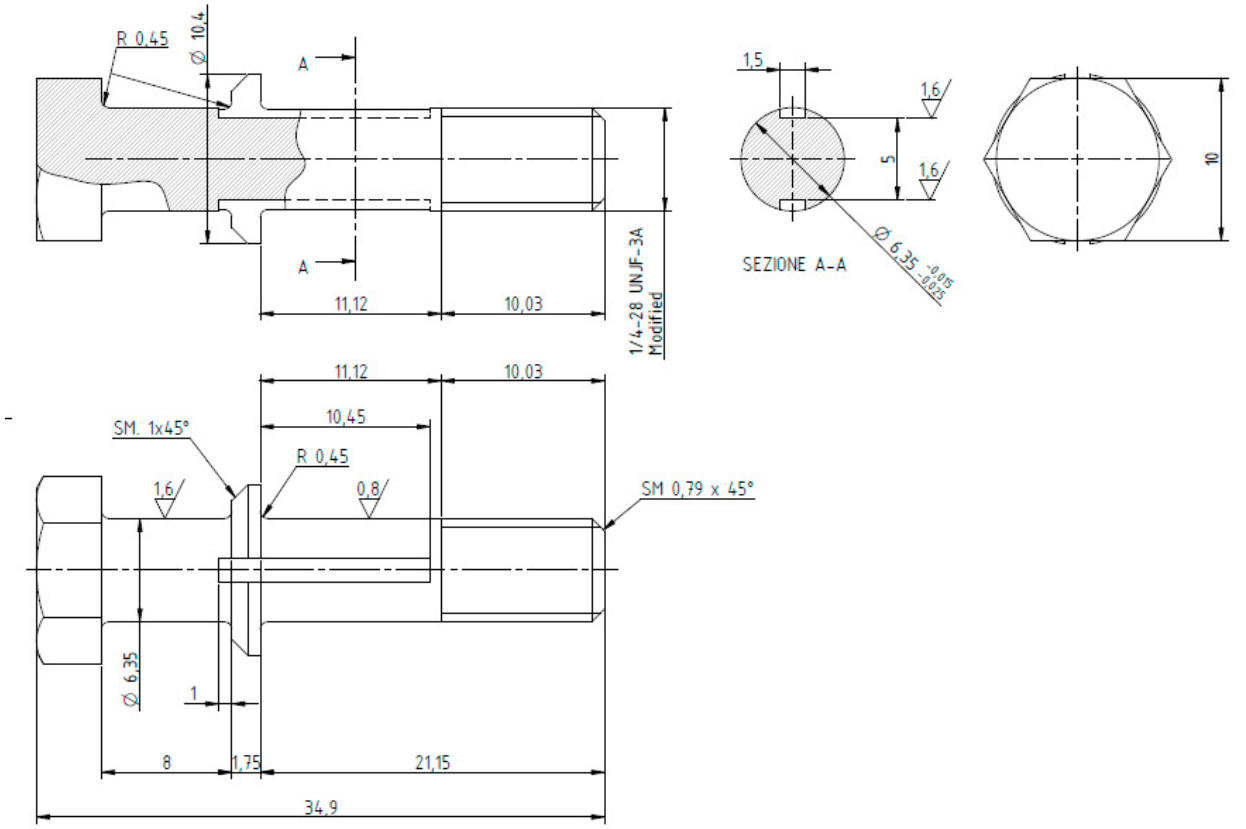

Fig. 3. Bolt geometry (dimensions in mm).

3. FE model

The numerical model of the joint has been developed by means of ABAQUS® code. The implicit formulation has been used for all performed analyses. The plates have been modelled by using the C3D8R linear hexahedral finite elements, from ABAQUS® library, having 8 nodes, with three translational degree of freedom for each node. The overlap zone, with a hole lodging the bolt, has been discretized with local different densities for better appreciating the stress and deformation states near to the joint (Fig. 4).

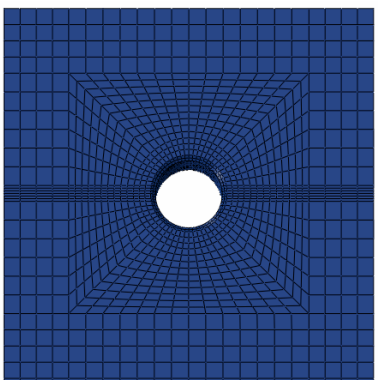

Fig. 4. Particular of the overlap zone of the plates.

The bolt and the nut have been modelled with C3D8R linear hexahedral elements too. Fig. 5a shows the mesh of the bolt. It is possible to observe a fine mesh density in correspondence of the shaft keyway. The nut (Fig. 5b) is a simple truncated circular cone with the mesh following the bolt one.

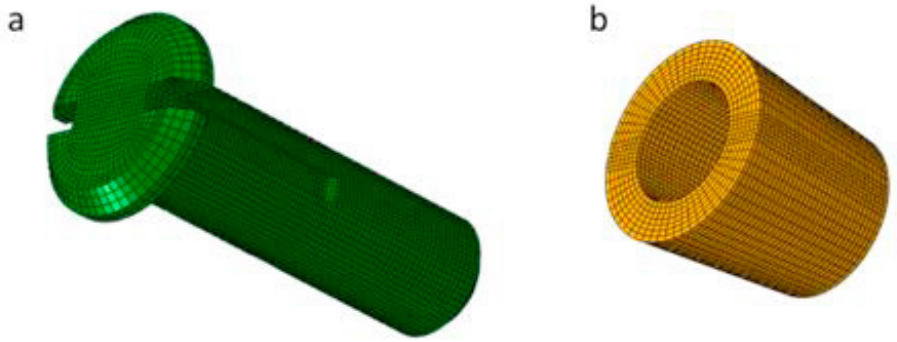

Fig. 5. FE models of bolt (a) and nut (b).

Fig. 6 shows the transversal section of the joint. A non-linear contact between the bolt and the plates was modelled based on the contact pair approach in ABAQUS with finite sliding allowed between surfaces in contact. A friction coefficient of 0.2 was assumed between plates and the bolt.

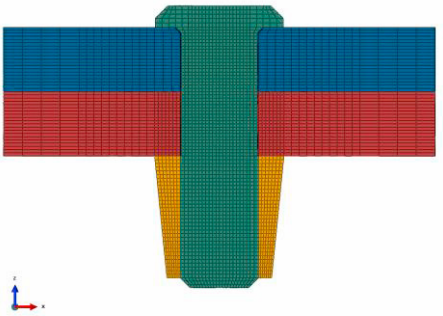

Fig. 6. Transversal section of the joint.

The whole FE model of the joint consists of 185572 elements and 203499 nodes.

3.1. Constrains and loads

Boundary conditions and loads have been modelled as shown in Fig. 7. The three degrees of freedom of nodes corresponding to the joint clamped end (left side of Fig. 7) have been completely constrained. While, the nodes on the opposite end (right side of Fig. 7) have been constrained in such a way to avoid displacements along x and z directions.

Regarding the loads, the preload of the bolt has been modelled by using pre-tension element implemented in ABAQUS®.

The external tensile load along y direction has been modelled as a concentrated load, applied on a multi-points constraint (left side of Fig. 7).

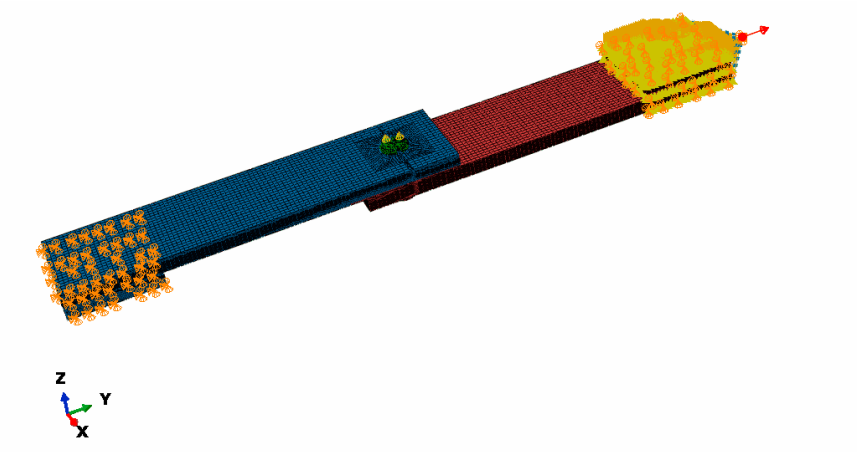

Fig. 7. Boundary and loading conditions.

4. Results

The stress field in a bolted single-lap joint is generally dependent on the tensile applied load and on the preload of the bolt.

In order to evaluate the behavior of the bolt under different loading conditions, this section describes the stress distributions under tensile stress load in two different cases:

1. tensile load applied without considering bolt preload;
2. tensile load applied considering bolt preload.

4.1. Stress distributions under tensile load without bolt preload

The behavior of the joint under tensile load F_y = 1000 N, without considering the preload of the bolt, has been simulated in order to understand how the shear stress is distributed.

Fig. 8 shows the component of shear stress τ_{zy} and τ_{zx} on the bolt up to the section in corresponding to the plates interface. It is possible to observe that the shear stress distribution is symmetric in the cross section and that the shear stress component τ_{zx} is negligible. Table 2 reports a comparison between average and maximum values obtained by Eq.(1) and Eq. (2) and numerical results.

$$\tau_{zy\_an} = \frac{F_y}{A} \tag{1}$$

$$\tau_{zy\_an} = \frac{4}{3} \cdot \frac{F_y}{A} \tag{2}$$

where F_y is the shear loading and A is the cross section of bolt.

Table 2. Shear stress τ_{zy} analytical/numerical values comparison at the section corresponding to the plates interface.

	τ_{zy_an} [MPa]	τ_{zy_num} [MPa]	Difference [%]
Average	33.6	29.8	11.3
Maximum	44.8	41.25	7.9

Following these observations, it is possible to state that whole tensile load is transferred to the bolt.

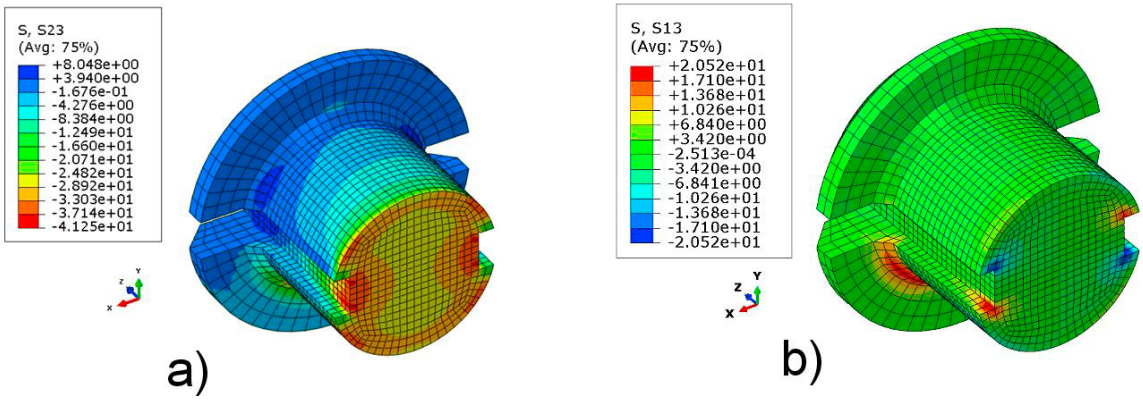

Fig. 8. Shear stress distribution in MPa on the bolt under applied tensile load of 1000 N, a) τ_{zy} shear component; b) τ_{zx} shear component.

Fig. 9 shows the stress distributions (σ_x , σ_y and σ_z) at section A-A (Fig. 1) and along transverse direction at plates interface. It is possible to observe that the transverse σ_x and longitudinal σ_y stresses assume significant values. The maximum value reached by σ_x is 8.25 MPa, while for σ_y, the maximum values is equal to 58.54 MPa in correspondence of the hole housing the bolt. About σ_z, it is possible to observe that it can be neglected since their values are almost zero.

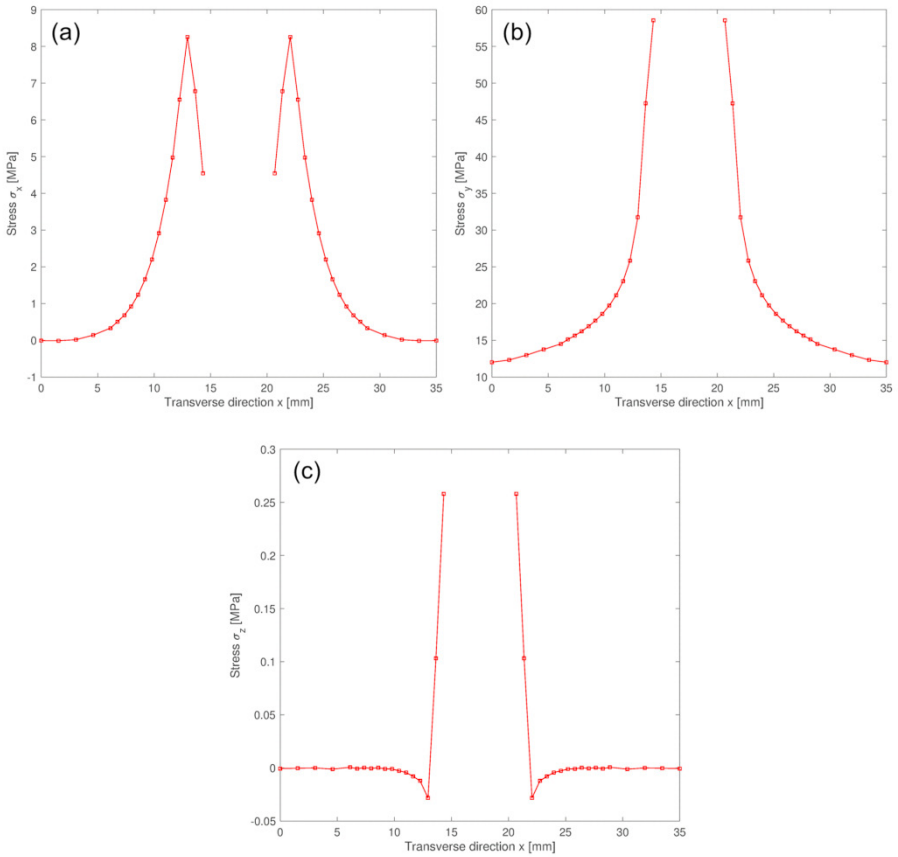

Fig. 9. Stress distributions σ_x (a), σ_y (b) and σ_z (c) at plates interfaces along transverse direction under only applied tensile load F_y = 1000 N.

4.2. Stress distribution under tensile load with bolt preload

The shear behavior of the bolt under both tensile load and preload condition has been simulated. In particular, by considering a tensile load F_y = 1000 N, the shear stress distributions on the bolt have been evaluated by varying the bolt preload.

Fig. 10 shows the shear stress τ_{zy} distributions on the bolt up to the section corresponding to the plates interface for several values of bolt preload, respectively equal to 500 N (Fig. 10.a), 1000 N (Fig 10.b), 1500 N (Fig. 10.c) and 2000 N (Fig. 10.d).

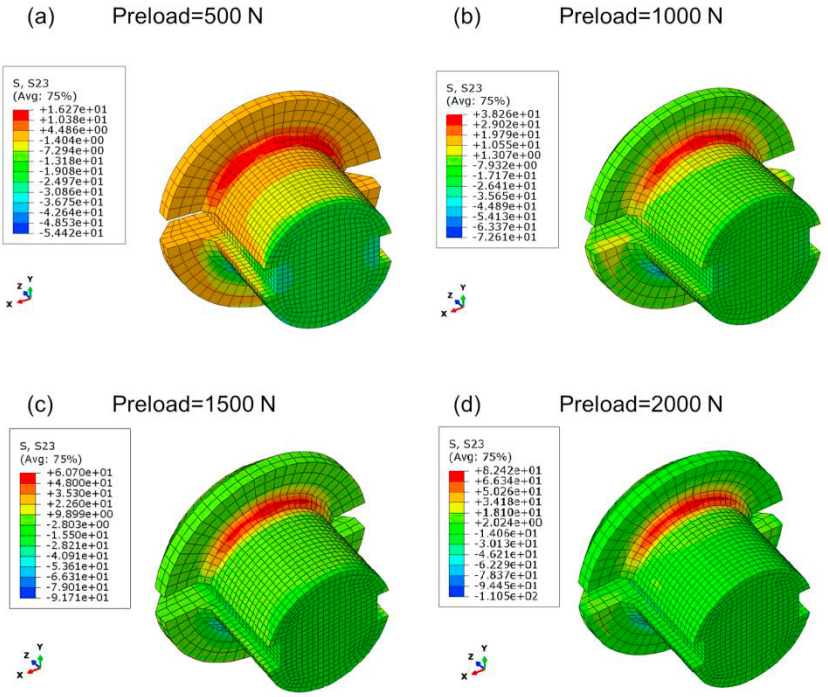

Fig. 10. Shear stress τ_{zy} distributions in MPa on the bolt under applied tensile load F_y = 1000 N by varying the bolt preload.

The average value of shear stress, τ_{zy} at the bolt section corresponding to the plates interface decreases as the preload increases (Fig. 11).

Therefore when the bolt is preloaded only one portion of tensile load is transferred to the bolt.

Regarding the stresses (σ_x, σ_y and σ_z) distributions along transverse direction at plates interface, several cases have been analyzed, assuming the following two conditions:

1. fixed bolt preload and variable tensile load;
2. fixed tensile load and variable bolt preload.

Concerning the bolt preload, the following values have been considered: 250 N, 500 N, 750 N, 1000 N, 1500 N and 2000 N.

About tensile load, the following values have been considered: 1000 N, 2500 N and 5000 N.

In this paper only some results of loading conditions studied were reported.

Fig. 12 shows the stress distributions σ_x (a, b), σ_y (c, d) and σ_z (e, f) at plates interfaces along transverse direction under two different preload conditions by varying the tensile load. The considered preload values are equal to 1000 N (Fig. 12.a, Fig. 12.c and Fig. 12.e) and to 2000 N (Fig. 12.b, Fig. 12.d and Fig. 12.f).

The most relevant values are reached by σ_x (Fig 12.a and Fig. 12.b) and σ_y (Fig. 12.c and Fig 12.d) respectively along transverse and longitudinal direction with respect to the applied tensile load. It is possible to observe that, at

fixed preload, the stresses σ_x and σ_y increase as the tensile load increases. By increasing the preload, in this case doubled, the stresses σ_x and σ_y values decrease. The maximum value reached by σ_y is in correspondence of the hole housing the bolt.

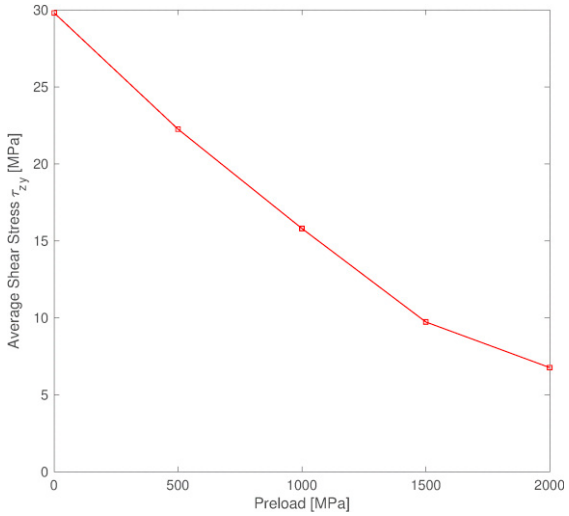

Fig. 11. Shear stress *τzy* trend as the bolt preload varies.

Regarding the stresses (σ_x, σ_y and σ_z) distributions along transverse direction at plates interface, several cases have been analyzed, assuming the following two conditions:

3. fixed bolt preload and variable tensile load;
4. fixed tensile load and variable bolt preload.

Concerning the bolt preload, the following values have been considered: 250 N, 500 N, 750 N, 1000 N, 1500 N and 2000 N.

About tensile load, the following values have been considered: 1000 N, 2500 N and 5000 N.

Fig. 12 and Fig. 13 show four of the analyzed cases.

Fig. 12 shows the stress distributions σ_x (a, b), σ_y (c, d) and σ_z (e, f) at plates interfaces along transverse direction under two different preload conditions by varying the tensile load. The considered preload values are equal to 1000 N (Fig. 12.a, Fig. 12.c and Fig. 12.e) and to 2000 N (Fig. 12.b, Fig. 12.d and Fig. 12.f).

The most relevant values are reached by σ_x (Fig 12.a and Fig. 12.b) and σ_y (Fig. 12.c and Fig 12.d) respectively along transverse and longitudinal direction with respect to the applied tensile load. It is possible to observe that, at fixed preload, the stresses σ_x and σ_y increase as the tensile load increases. By increasing the preload, in this case doubled, the stresses σ_x and σ_y values decrease. The maximum value reached by σ_y is in correspondence of the hole housing the bolt.

About σ_z (Fig. 12.e and Fig. 12.f), the values the values are not particularly influenced by the variation of tensile load and can be considered negligible compared to σ_x and σ_y.

Fig. 13 shows the stress distributions σ_x (a, b), σ_y (c, d) and σ_z (e, f) at plates interfaces along transverse direction under two different tensile load conditions by varying the preload. The considered tensile load values are equal to 1000 N (Fig. 13.a, Fig. 13.c and Fig. 13.e) and to 2500 N (Fig. 13.b, Fig. 13.d and Fig. 13.f).

In addition, the most relevant values are reached by σ_x (Fig 13.a and Fig. 13.b) and σ_y (Fig. 13.c and Fig 13.d) respectively along transverse and longitudinal direction with respect to the applied tensile load. It is possible to observe that, at fixed tensile load, the stresses σ_x and σ_y decrease as the preload increases. This behavior is confirmed also by increasing the tensile load. The maximum value reached by σ_y is in correspondence of the hole housing the bolt.

About σ_z (Fig. 13.e and Fig. 13.f), it is not particularly influenced by the increment of tensile load while its values decrease as the preload increases.

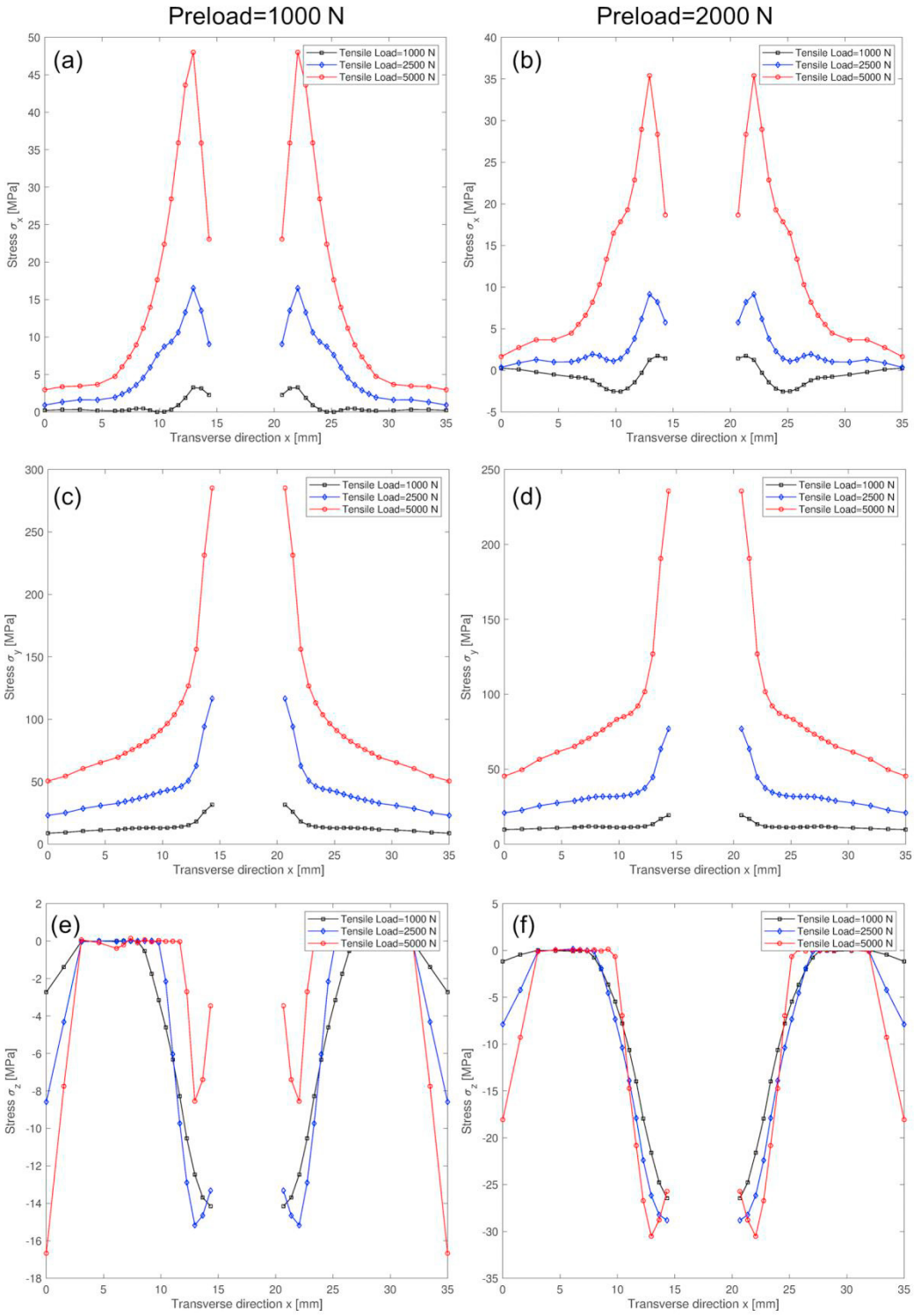

Fig. 12. Stress distributions σ_x (a, b), σ_y (c, d) and σ_z (e, f) at plates interfaces along transverse direction under two different pre-load conditions by varying the tensile load.

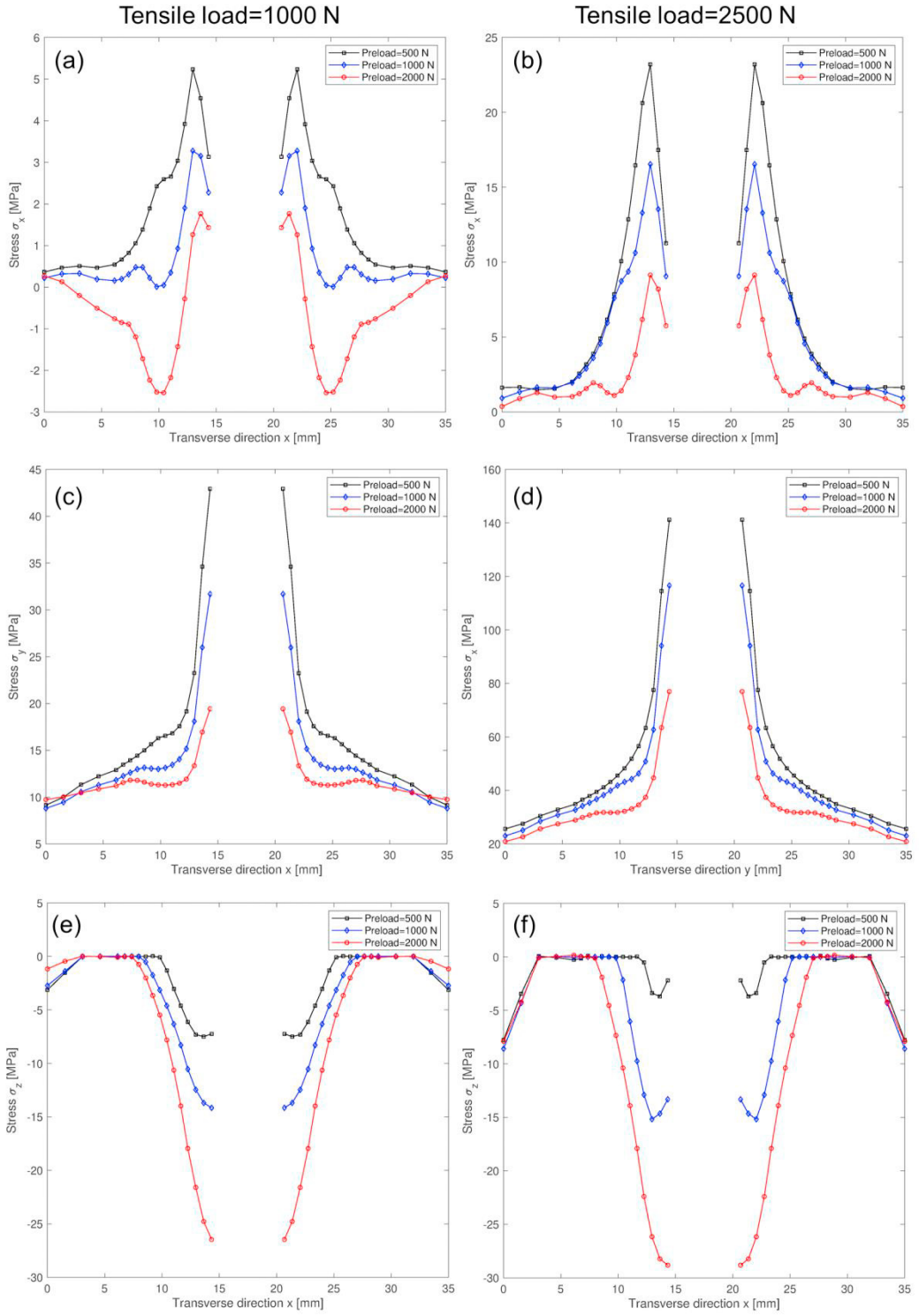

Fig. 13. Stress distributions σ_x (a, b), σ_y (c, d) and σ_z (e, f) at plates interfaces along transverse direction under two different tensile-load conditions by varying the pre-load.

5. Conclusions

A FE model aimed to simulate the mechanical behavior of a bolted single-lap joint has been realized in order to support the design phase of strain gauges instrumented bolt.

The results analysis shows that the numerical model is able to predict the mechanical behavior of the joint and that the bolt preload influences the stress distributions under real loading conditions.

In particular, the stress distributions have been evaluated under two main conditions: the former, which not considers the bolt preload (only the tensile load is modelled); the latter, where both tensile load and bolt preload conditions have been modelled.

In the first condition, that considers the only tensile load, by comparing the analytical and numerical results, it has been demonstrated that the tensile load applied to the joint is completely transferred to the bolt.

In the second condition, the results showed how the tensile load transferred to the bolt decreases almost linearly as the preload increases.

Concerning the transverse and longitudinal stresses (with respect to the tensile load direction) at the plates interfaces, the results demonstrated how the preload influences their distributions. Indeed, at a selected preload level, both transverse and longitudinal stresses increase as the tensile load increases while, at a selected tensile load, they decrease as the preload level increases.

References

Aldaş K, Sen F., 2013. Stress analysis of hybrid joints of metal and composite plates via 3D-FEM. Indian Journal of Engineering & Material Sciences 20, 92-100.

Armentani E, Laiso M., Caputo F., Sepe R., 2018. Numerical FEM Evaluation for the Structural Behaviour of a Hybrid (bonded/bolted) Single-lap Composite Joint. Procedia Structural Integrity 8, 137-153.

Atta M., Abd-Elhady A.A., Abu-Sinna A., Sallam H.E.M., 2019. Prediction of failure stages for double lap joints using finite element analysis and artificial neural networks. Engineering Failure Analysis 97, 242-257.

Barut A., Madenci E., 2009. Analysis of bolted-bonded composite single-lap joints combined in-plane and transverse loading. Composite Structures 88, 579-594.

Bois C., Wargnier H., Wahl J.C., Le Goff E., 2013. An analytical model for the strength prediction of hybrid (bolted/bonded) composite joints. Composite Structures 97, 252-260.

Chakherlou T.N., Abazadeh B., 2011. Investigating clamping force variation in Al2024-T3 interference fitted bolted under static and cyclic loading. Material design 37, 128-136.

Chakherlou T.N., Razavi M.J., Aghdam A.G., Abazadeh B., 2012. An experimental investigation of the bolt clamping force and friction effect on the fatigue behavior of aluminum alloy 2024-T3 double shear lap joint. Material design 32, 4641-4649.

De Luca A., Greco A., Armentani E., Sepe R., Caputo F., 2018. Numerical and experimental evaluation of stress relaxation in hybrid composite-metal bolted joints. AIP Conference Proceedings 1981.

He X., 2011. A review of finite element analysis of adhesively bonded joints. International Journal of Adhesion & Adhesive 31, 248-264.

Hoang-Ngoc C.T., Paroissien E., 2010. Simulation of single-lap bonded and hybrid (bolted/bonded) joints with flexible adhesive. International Journal of Adhesion & Adhesives 30, 117-129.

Kelly G., 2005. Load transfer in hybrid (bonded/bolted) composite single-lap composite joints. Composite Structures 43, 195-216.

Kelly G., 2006. Quasi-static strength and fatigue life of hybrid (bonded/bolted) composite single-lap joints. Composite Structures 72, 119-129.

Lamanna, G., 2014. Tensile testing of hybrid composite joints. Applied Mechanics and Materials 575, 452-456.

McCarthy M.A., McCarthy C.T., Lawlor V.P., Stanley W.F., 2005. Three-dimensional finite element analysis of single-bolt, single-lap composite bolted joints: part I-model development and validation.

Samaei M., Zehsaz M., Chakherlou T.N., 2016. Experimental and numerical study of fatigue crack growth of aluminum alloy 2024-T3 single lap simple bolted and hybrid (adhesive/bolted) joints. Engineering Failure Analysis 59, 253-268.

Sawa S., Ishimura M., Sekiguchi Y., Sawa T., 2015. FEM stress analysis and design for bolted circular flange joints under tensile loading. Proceedings of ASME 2015 IMECE2015-50576.

Shirakawa A., Sawa T., Naruse T., 2018. FEM contact stress analysis at the bearing surfaces in bolted joints under external loadings. Proceedings of the ASME 2018 PVP2018-84086.